Piezoelectric Nanofibers for Non-Invasive Wearable Blood Pressure Monitoring

Andrew Closson[1], Zhe Xu[1], Jessica Bargamian[2], Alessandra Bryan[2], Alexander Abess[2], John X.J. Zhang[1*]
[1]Thayer School of Engineering, Dartmouth College, Hanover, NH, 03755, USA
[2]Dartmouth Hitchcock Medical Center, Lebanon, NH, 03766, USA
*Corresponding author Email: John.Zhang@Dartmouth.edu

Abstract

We present a study on the development of piezoelectric nanofibers for wearable hemodynamic sensing by incorporating nanoparticle doping of piezoelectric nanofibers. The composite material was characterized using various techniques, including scanning electron microscopy, X-ray diffraction, and tensile test. The material was also evaluated in a custom-built pressure chamber. Achieving optimal sensor performance, the study identified 20 wt% BTO composite materials as ideal, with a peak voltage output of 0.12V. Higher concentrations presented electrospinning difficulties, compromising material consistency. Quantitative analysis through fast Fourier transform (FFT) and digital bandpass filtering precisely isolated physiological signals, notably respiration and heartbeat, with the sensor demonstrating accurate detection capabilities at frequencies of 0.2, 1.35, and 2.65 Hz, indicative of the targeted physiological processes. The results demonstrate a promising potential for the use of these materials in future wearable hemodynamic sensing applications.

Keywords: piezoelectric nanofibers, composite, electrospinning, wearable sensor, blood pressure monitoring

Introduction

With the rise of chronic diseases and an aging population, non-invasive monitoring of hemodynamic parameters such as blood pressure has become increasingly important. Current methods for blood pressure monitoring, one example being oscillometry, are either invasive or require bulky equipment, limiting their use for continuous and remote monitoring. Wearable devices that can accurately and conveniently monitor blood pressure would have significant implications for healthcare and medical research for the 116 million Americans who have hypertension [1]. With the potential to seamlessly integrate with the human body, these sensors could provide detailed information about health and habits.

Recent studies have investigated wearable sensors for non-invasive monitoring of heart rate and blood pressure[2,3]. Optical devices can potentially detect pulse wave velocity[4,5], diastolic and systolic blood pressure[6,7], pulse oximetry[8], and cardiac output[9]. Machine and deep learning have shown significant promise in this area, although their application in piezoelectric devices remains unexplored[10].

Piezoelectric materials, which convert mechanical pressure into electrical signals, are promising for flexible, ultra-low-pressure sensing. Polyvinylidene fluoride (PVDF) and its copolymers are potentially useful but need enhanced sensitivity. Techniques like electrospinning [11–15] and material doping [16–24] have been used to create these sensors due to their simplicity and ability to yield high-quality, customizable nanofibers.

In this paper, we present a study on the development of piezoelectric nanofibers for wearable hemodynamic sensing. We focus on nanoparticle doping of piezoelectric and conductive nanofibers to improve their piezoelectric and electrical properties, as well as characterize the materials using various techniques. We also test the materials in a custom-built pressure chamber

to evaluate their sensitivity. We further review methods for using wearable sensors for cuffless blood pressure monitoring and propose an approach that makes use of the previously developed materials. Finally, we demonstrate the potential for wearable blood pressure monitoring with a human study comparing piezoelectric sensor outputs to gold standard invasive arterial blood pressure catheters.

Results and Discussion

Piezoelectric nanoparticle doping of polyvinylidene fluoride (PVDF) and its copolymer poly(vinylidene fluoride-co-trifluoroethylene) (P(VDF-TrFE)) has been shown to improve the piezoelectric properties of the material[25,26]. Barium titanate (BTO) is of interest for human interfacing applications due to its biocompatibility[27–29]. When it is incorporated into PVDF, it enhances the overall piezoelectric response of the composite material due to its comparatively high piezoelectric constant[30,31]. Additionally, BTO nanoparticles also help to align the PVDF molecules in a preferred direction that encourages the formation of the piezoelectric crystalline β-phase[32].

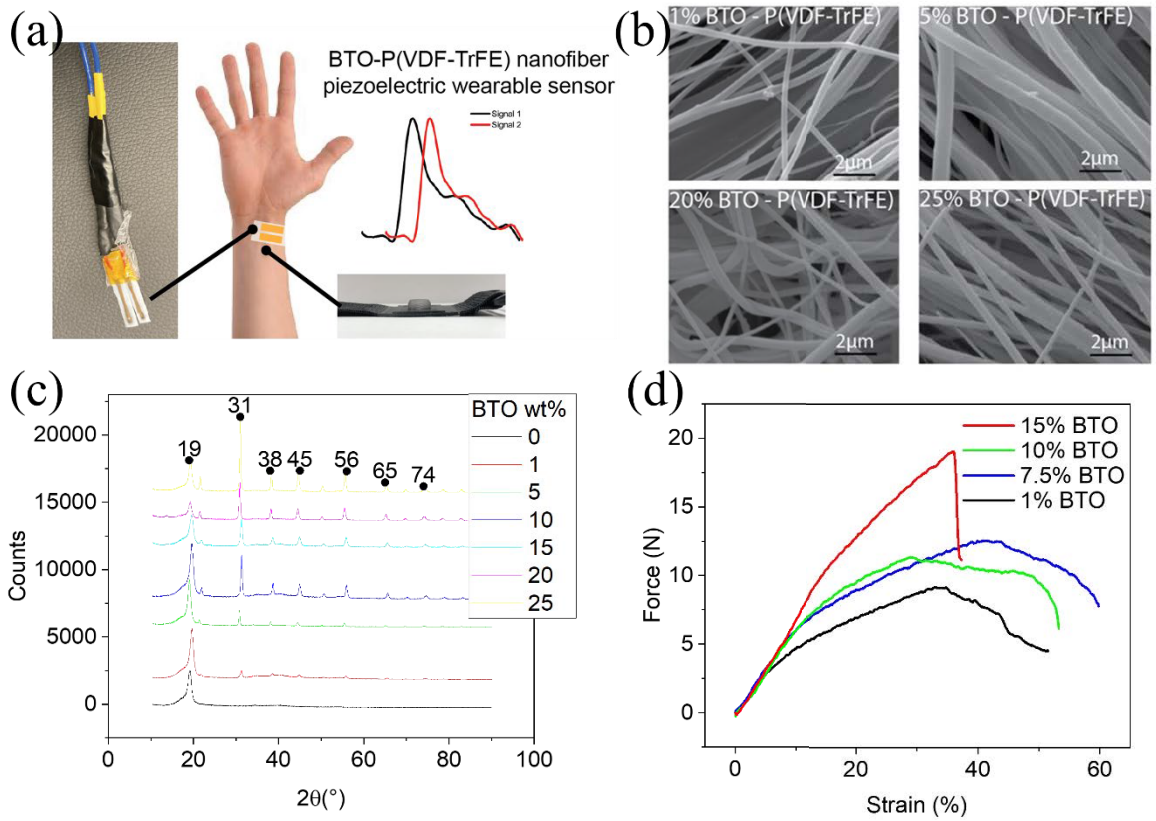

Figure 1: (a) a piezoelectric sensor on a wristband placed over the radial artery (b) SEM images of the varying wt% of BTO doped into PVDF-TrFE nanofibers. (c) XRD of varying wt% BTO doped into PVDF-TrFE nanofibers. (d) Tensile test of varying wt% BTO doped into PVDF-TrFE nanofibers.

In Figure 1(a), the schematic demonstrates that the piezo sensor made of BTO doped P(VDF-TrFE) nanofiber placed over the radial artery and secured with a Velcro wristband. Embedded in the wrist strap was a raised hemisphere of soft silicone that was placed on top of the piezoelectric

array sensor (PAS) to provide backing pressure that improves signal output. From the material aspect, we investigated the doping of BTO in wt% 0-25 into P(VDF-TrFE) to form composite nanofibers via electrospinning. **Figure 1(b)** shows top-down SEM images of representative fibers for 1, 5, 20, and 25 wt% BTO- P(VDF-TrFE). BTO nanoparticles (45nm) can be seen as rough, granular surfaces in all four images and they become more concentrated with higher doping percentage. X-ray diffraction (XRD) was used to characterize the crystalline properties of the composite materials compared to pristine P(VDF-TrFE) nanofibers, **Figure 1(c)**. The pristine P(VDF-TrFE) shows its characteristic peak at ~19° while the characteristic BTO peak (31, 38, 45, 56, 65, 74 °) become more prevalent at higher doping wt%. The effect of the dopant's concentration on strength of the composite material was characterized using a tensile test (Instron), **Figure 1(d)**. The Young's modulus increases with increasing BTO wt%.

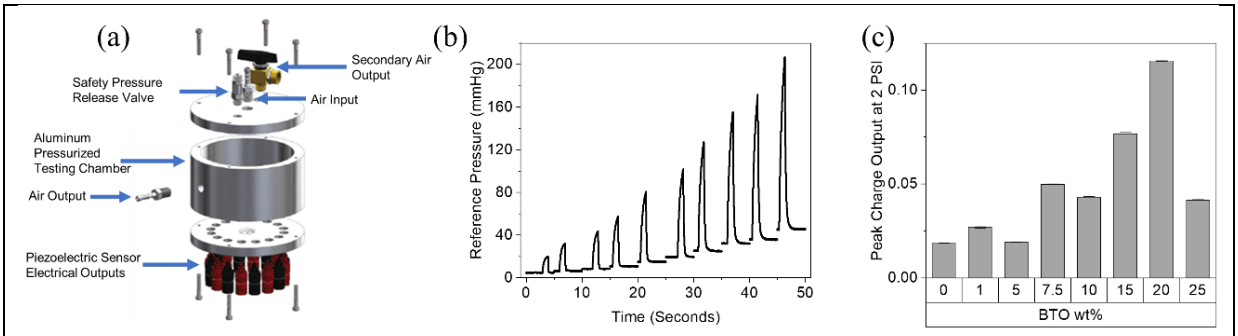

Figure 2: (a) 3D exploded view of the pressure sensing test chamber used to characterize the double-doped core-shell nanofibers. (b) A pressure sweep showing the range of possible applied pressures by the test system. (c) Peak charge outputs from a 2 psi pressure input on PVDF-TrFE nanofibers doped with varying wt% of BTO.

We used a custom-built pressure sensor test chamber (**Figure 2(a)**) to characterize the BTO doped P(VDF-TrFE) nanofibers as potential pressure sensors. The aluminum chamber had a physiologically relevant input pressure from 0-210 mmHg, adjusted with a solenoid valve controlled by an Arduino microcontroller. **Figure 2(b)** shows a sweep of potential input pressure from 0 to 210 mmHg. The with timed opening and closings of the output solenoid valve it is possible to apply periodic pressure impulses onto the BTO-doped P(VDF-TrFE) nanofibers. **Figure 2(c)** shows the peak charge outputs of the composite materials with a 2 psi input pressure. The outputs show an expected increasing trend to a maximum at 20 wt% BTO and the peak voltage is 0.12V. The 25 wt% BTO was expected to have a larger output, but we believe the discrepancy is due to poor electrospinning performance of the higher wt% solution. At 25 wt%, the BTO-P(VDF-TrFE) solution became very viscous and the appearance of the Taylor cone was intermittent, leading to sparse fiber formation. For this reason, 20 wt% BTO-P(VDF-TrFE) was chosen as the material composition for the rest of the study.

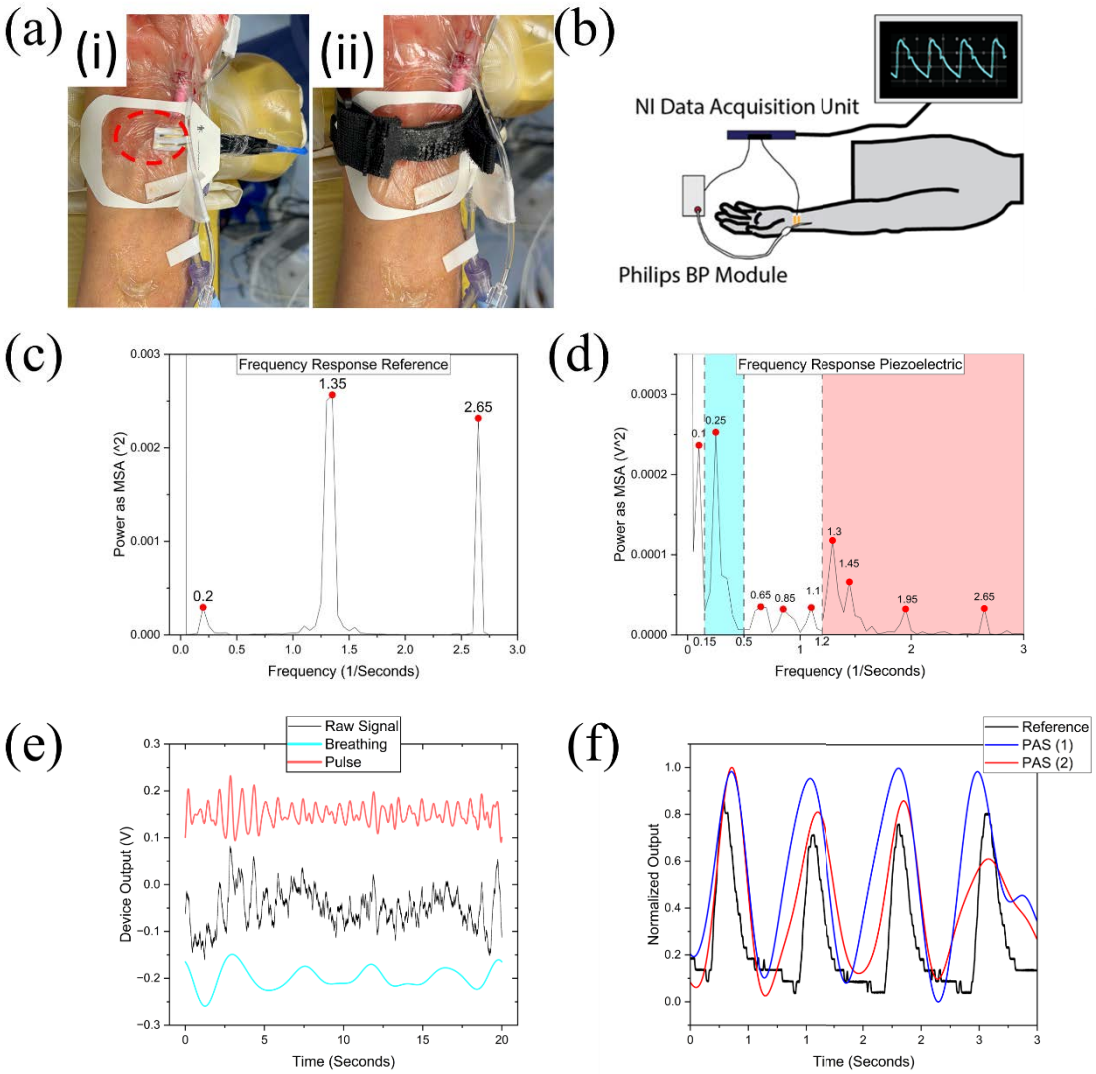

Figure 3: (a) a piezoelectric sensor tested in clinical setting; (b) an in-vivo test using an arterial line pressure catheter for continuous blood pressure reference; (c) the frequency response of the arterial line sensor; (d) the frequency response of the sensor, highlighting respiration (blue) and pulse (red) ranges; (e) comparison of the raw and filtered signals producing breath (blue) and heartbeat (red) waveforms; (f) a comparison of normalized signals from the reference sensor and the piezoelectric sensor elements.

We tested a 2x1 element array of composite nanofiber as a flexible piezoelectric blood pressure sensor in clinical setting in **Figure 3(a)**. **Figure 3(a-i)** displays the sensor placed over the radial artery and temporarily secured by a 3M medical tape. The location of the senor is highlighted by the red dash circle. Then in **Figure (a-ii)**, the sensor is secured with a home designed velcro wristband. **Figure 3(b)** illustrates the test setup. An arterial line catheter, placed proximally on the same artery, serves as the gold standard measurement. Signals from the piezoelectric sensor and reference blood pressure are recorded via a National Instruments DAQ and a Philip's module respectively. The device's feasibility was confirmed on a single patient, with data collected to

develop and test blood pressure estimation algorithms.

A 20-second high-quality data sample was analyzed using a fast Fourier transform (FFT) to study the frequency of both the reference and piezoelectric signals (**Figures 3(c) and 3(d)**). The reference signal displayed three key peaks under 3 Hz (0.2, 1.35, 2.65 Hz), representing respiration, heartbeat, and the second heartbeat harmonic respectively. The piezoelectric signal had more peaks but preserved respiration and heartbeat signals. Two digital bandpass filters were created to separate respiration (0.15-0.5 Hz) and heartbeat (1.2-4 Hz). **Figure 3(e)** presents the filter effects, while **Figure 3(f)** compares processed PAS and raw reference signals, indicating a good overlap.

Conclusion and Future Directions

In this study, we've enhanced P(VDF-TrFE) piezoelectric nanofibers' properties with barium titanate and multi-walled carbon nanotubes for wearable blood pressure sensing in the pursuit of optimizing the performance of implantable bioelectronic sensors, our research has illuminated critical findings on material composition and signal processing capabilities. The investigation into the composite materials' peak charge outputs under a 2 psi input pressure revealed a notable trend: an optimal sensor performance was achieved with a composition of 20 wt% Barium Titanate (BTO), which produced a peak voltage of 0.12V. Interestingly, while an increase to 25 wt% BTO was anticipated to yield higher outputs, the results fell short of expectations due to compromised electrospinning performance at higher concentrations. The increased viscosity at 25 wt% BTO-P(VDF-TrFE) resulted in inconsistent fiber formation, highlighting the delicate balance between material composition and manufacturing processes. Consequently, 20 wt% BTO-P(VDF-TrFE) was determined as the optimal material composition for further development in this study.

Wearable blood pressure sensors have transformative potential for non-invasive, continuous hemodynamic monitoring. A detailed examination of a 20-second high-quality data sample using fast Fourier transform (FFT) enabled the differentiation of key physiological signals—namely, respiration and heartbeat—within the reference and piezoelectric signals. The reference signal identified three significant peaks below 3 Hz, corresponding to respiration, heartbeat, and the second heartbeat harmonic, establishing a benchmark for physiological monitoring. Through the implementation of two digital bandpass filters designed to isolate respiration (0.15-0.5 Hz) and heartbeat (1.2-4 Hz) signals, we demonstrated the sensor's capability to accurately capture and process physiological data. The effective comparison of processed and raw signals further validated the sensor's potential in providing reliable and precise health monitoring.
Despite promising progress, integrating these materials into wearable devices needs more research. We foresee further development in machine learning improving blood pressure monitoring accuracy and reliability.

Overall, the development of wearable sensors for blood pressure monitoring has the potential to revolutionize the field of hemodynamic sensing by providing continuous and non-invasive blood pressure monitoring. The use of piezoelectric nanofibers is a promising approach to improving the sensitivity and selectivity of these sensors. However, the integration of these materials into wearable devices is still a developing field and requires further research. We anticipate that the ongoing development of wearable sensors and machine learning algorithms will continue to improve the accuracy and reliability of blood pressure monitoring in the future.

Materials and experiments

Electrospinning BTO doped P(VDF-TrFE) nanofiber: 45 nm cubic Barium titanate (BTO) (Sigma-Aldirch) were dissolved in a 2:1 volume ratio mixture of N,N-dimethylformamide (DMF) and Butanone (MEK) solvent, both purchased from Sigma-Aldrich, at varying wt% and mixed under magnetic stirring for 10 minutes. P(VDF-TrFE) 75:25 powder (Piezotech) was then added at 18 wt%. The final mixture was mixed under magnetic stirring for 4 hours in a water bath at 60 °C. The solution was electrospun using a 20-gauge needle, a flow rate of 1.5 ml/hr, and an applied voltage of 16 kV. A rotating drum collector was used to create aligned fibers, at a distance of 11 cm from the needle, and a rotation speed of 3,000 rpm. Due to the in-situ poling, no further electrical poling or thermal annealing processes were required. The BTO doped P(VDF-TrFE) fiber mat was removed from the collection drum as a standalone free film using a razor blade.

Electrode Deposition: Next, a thin filler layer of polydimethylsiloxane (PDMS), diluted in tert-Butyl alcohol (TBA) in a 1:1 v/v ratio, was spin coated for 1 minute at 1000 rpm onto the BTO doped P(VDF-TrFE) fiber mat. The mat was then heated in the oven for 1 hour at 90°C to cure the PDMS. Gold electrodes (20 nm) were then magnetron sputter coated on the top and bottom of the piezoelectric thin film to form a functional piezoelectric sensor.

Device wiring and encapsulation: For pressure testing and human subject validation testing, 29-gauge wires were bonded to each electrode using silver paint and Kapton tape. The device was then dip coated in PDMS to encapsulate the electrodes and further secure the wires. The PDMS was then cured in the oven for 1 hour at 90°C. The wires were soldered to a stripped low noise coaxial cable (PCB Piezotronics) and further shielded with a wrapping of aluminum foil and heat-shrink tubing.

Tensile tests: To characterize the mechanical strength of the fiber mats a tensile extension test was used (Instron). Samples of similar thickness were cut into dog-bone shapes of specified dimensions. The extension rate was set to 10 mm/min.

Crystallography: Crystalline phase identification of BTO doped P(VDF-TrFE) fibers was measured by x-ray diffraction (XRD) using a Rigaku D/MAX 2000 with Cu-Kα radiation. The 2θ range was from 10° to 90° with a scanning speed of 1° min^{-1}.

Human subject validation experimental method: The human subject validation experiment compared a reference continuous blood pressure to the voltage output measured by the PAS. The study was done in partnership with Dartmouth Hitchcock Medical Center (STUDY02001549). The only deviations from routine clinical care include application of the PAS to the study participant during their surgical procedure. The PAS was placed on the skin overlying the radial artery and secured in place with a Tegaderm or other similar medically approved adhesive tape. A wrist strap with soft silicone dome was lightly wrapped over the sensor to provide backing pressure. The strap was loosened and reset each hour. The second PAS also used a wrist strap to provide backing pressure. Immediately prior to placement of the PA, the depth from skin to the radial artery was measured by ultrasound. This measurement serves to inform the PAS performance characteristics in case artery-to-skin distance is an important determinant of device performance. The PAS was connected to data collection equipment (PCB Piezotronics) that is electrically isolated from the patient such that there is no risk of electrical shock. The PAS was applied to the study participant after the clinical team placed the intended invasive arterial pressure monitoring catheter (radial artery catheter). The PAS was placed in a location that is close to the radial artery catheter, but it did not interfere

with clinical team caring for the study participant. Output from piezoelectric array sensor was recorded using a National Instruments data acquisition unit (National Instruments)) and logged with a customized LabView program. Reference BP data was also measured with the same data acquisition unit via a Philips M1006B Invasive Blood Pressure Measurement Module.

Acknowledgments

The authors acknowledge the financial support from the National Institute of Health (NIH) Exploratory/Developmental Grant Program (NIH/NIBIB 1R21EB032056) and the NH EPSCoR NH BioMade Project is provided by the National Science Foundation's Research Infrastructure Improvement Award # 1757371.

References

(1) Ostchega, Y.; Fryar, C. D.; Nwankwo, T.; Nguyen, D. T. Hypertension Prevalence among Adults Aged 18 and over: United States, 2017–2018. **2020**.

(2) Liu, Z.-D.; Liu, J.-K.; Wen, B.; He, Q.-Y.; Li, Y.; Miao, F. Cuffless Blood Pressure Estimation Using Pressure Pulse Wave Signals. *Sensors* **2018**, *18* (12), 4227.

(3) Kim, J.; Chou, E.; Le, J.; Wong, S.; Chu, M.; Khine, M. Soft Wearable Pressure Sensors for Beat-to-beat Blood Pressure Monitoring. *Adv Healthc Mater* **2019**, *8* (13), 1900109.

(4) Zieff, G.; Stone, K.; Paterson, C.; Fryer, S.; Diana, J.; Blackwell, J.; Meyer, M. L.; Stoner, L. Pulse-Wave Velocity Assessments Derived from a Simple Photoplethysmography Device: Agreement with a Referent Device. *Front Cardiovasc Med* **2023**, *10*, 1108219.

(5) Van Velzen, M. H. N.; Niehof, S. P.; Mik, E. G.; Loeve, A. J. Measuring Pulse Wave Velocity with a Novel, Simple Sensor on the Finger Tip: A Feasibility Study in Healthy Volunteers. *Biomed Phys Eng Express* **2019**, *5* (6), 065010.

(6) Hosanee, M.; Chan, G.; Welykholowa, K.; Cooper, R.; Kyriacou, P. A.; Zheng, D.; Allen, J.; Abbott, D.; Menon, C.; Lovell, N. H. Cuffless Single-Site Photoplethysmography for Blood Pressure Monitoring. *J Clin Med* **2020**, *9* (3), 723.

(7) Natarajan, K.; Block, R. C.; Yavarimanesh, M.; Chandrasekhar, A.; Mestha, L. K.; Inan, O. T.; Hahn, J.-O.; Mukkamala, R. Photoplethysmography Fast Upstroke Time Intervals Can Be Useful Features for Cuff-Less Measurement of Blood Pressure Changes in Humans. *IEEE Trans Biomed Eng* **2021**, *69* (1), 53–62.

(8) Schlesinger, O.; Vigderhouse, N.; Moshe, Y.; Eytan, D. Estimation and Tracking of Blood Pressure Using Routinely Acquired Photoplethysmographic Signals and Deep Neural Networks. *Crit Care Explor* **2020**, *2* (4), e0095.

(9) Lee, Q. Y.; Redmond, S. J.; Chan, G. S. H.; Middleton, P. M.; Steel, E.; Malouf, P.; Critoph, C.; Flynn, G.; O'Lone, E.; Lovell, N. H. Estimation of Cardiac Output and Systemic Vascular Resistance Using a Multivariate Regression Model with Features Selected from the Finger Photoplethysmogram and Routine Cardiovascular Measurements. *Biomed Eng Online* **2013**, *12*, 1–15.

(10) Tamura, T. Current Progress of Photoplethysmography and SPO2 for Health Monitoring. *Biomed Eng Lett* **2019**, *9* (1), 21–36.

(11) Xue, J.; Wu, T.; Dai, Y.; Xia, Y. Electrospinning and Electrospun Nanofibers: Methods, Materials, and Applications. *Chem Rev* **2019**, *119* (8), 5298–5415.

(12) Haider, A.; Haider, S.; Kang, I.-K. A Comprehensive Review Summarizing the Effect of Electrospinning Parameters and Potential Applications of Nanofibers in Biomedical and Biotechnology. *Arabian Journal of Chemistry* **2018**, *11* (8), 1165–1188.

(13) He, Z.; Rault, F.; Lewandowski, M.; Mohsenzadeh, E.; Salaün, F. Electrospun PVDF Nanofibers for Piezoelectric Applications: A Review of the Influence of Electrospinning Parameters on the β Phase and Crystallinity Enhancement. *Polymers (Basel)* **2021**, *13* (2), 174.

(14) Huang, Z.-M.; Zhang, Y.-Z.; Kotaki, M.; Ramakrishna, S. A Review on Polymer Nanofibers by Electrospinning and Their Applications in Nanocomposites. *Compos Sci Technol* **2003**, *63* (15), 2223–2253.

(15) Kalimuldina, G.; Turdakyn, N.; Abay, I.; Medeubayev, A.; Nurpeissova, A.; Adair, D.; Bakenov, Z. A Review of Piezoelectric PVDF Film by Electrospinning and Its Applications. *Sensors* **2020**, *20* (18), 5214.

(16) Anh, D. P.; Tung, V. T. Preparation and Characterization of PZT/PVDF Composites Films Fabricated by Electrospinning Method. *arXiv preprint arXiv:2004.06928* **2020**.

(17) Sharafkhani, S.; Kokabi, M. High Performance Flexible Actuator: PVDF Nanofibers Incorporated with Axially Aligned Carbon Nanotubes. *Compos B Eng* **2021**, *222*, 109060.

(18) Kaspar, P.; Sobola, D.; Částková, K.; Dallaev, R.; Šťastná, E.; Sedlák, P.; Knápek, A.; Trčka, T.; Holcman, V. Case Study of Polyvinylidene Fluoride Doping by Carbon Nanotubes. *Materials* **2021**, *14* (6), 1428.

(19) Kim, S.-R.; Yoo, J.-H.; Park, J.-W. Using Electrospun AgNW/P (VDF-TrFE) Composite Nanofibers to Create Transparent and Wearable Single-Electrode Triboelectric Nanogenerators for Self-Powered Touch Panels. *ACS Appl Mater Interfaces* **2019**, *11* (16), 15088–15096.

(20) Xu, Z.; Jin, C.; Cabe, A.; Escobedo, D.; Hao, N.; Trase, I.; Closson, A. B.; Dong, L.; Nie, Y.; Elliott, J. Flexible Energy Harvester on a Pacemaker Lead Using Multibeam Piezoelectric Composite Thin Films. *ACS Appl Mater Interfaces* **2020**, *12* (30), 34170–34179.

(21) Jin, C.; Hao, N.; Xu, Z.; Trase, I.; Nie, Y.; Dong, L.; Closson, A.; Chen, Z.; Zhang, J. X. J. Flexible Piezoelectric Nanogenerators Using Metal-Doped ZnO-PVDF Films. *Sens Actuators A Phys* **2020**, *305*, 111912.

(22) Panwar, L. S.; Panwar, V.; Anoop, G.; Park, S. Carbon Nanofiber-Polyelectrolyte Triggered Piezoelectric Polymer-Based Hydrophilic Nanocomposite for High Sensing Voltage Generation. *Journal of Materials Research and Technology* **2022**, *17*, 3246–3261.

(23) Nivedhitha, D. M.; Jeyanthi, S. Polyvinylidene Fluoride, an Advanced Futuristic Smart Polymer Material: A Comprehensive Review. *Polym Adv Technol* **2023**, *34* (2), 474–505.

(24) Yun, J. S.; Park, C. K.; Jeong, Y. H.; Cho, J. H.; Paik, J.-H.; Yoon, S. H.; Hwang, K.-R. The Fabrication and Characterization of Piezoelectric PZT/PVDF Electrospun Nanofiber Composites. *Nanomaterials and Nanotechnology* **2016**, *6*, 20.

(25) Liu, M.; Liu, Y.; Zhou, L. Novel Flexible PVDF-TrFE and PVDF-TrFE/ZnO Pressure Sensor: Fabrication, Characterization and Investigation. *Micromachines (Basel)* **2021**, *12* (6), 602.

(26) Hu, X.; Yan, X.; Gong, L.; Wang, F.; Xu, Y.; Feng, L.; Zhang, D.; Jiang, Y. Improved Piezoelectric Sensing Performance of P (VDF–TrFE) Nanofibers by Utilizing BTO Nanoparticles and Penetrated Electrodes. *ACS Appl Mater Interfaces* **2019**, *11* (7), 7379–7386.

(27) Park, J. B.; Kelly, B. J.; Kenner, G. H.; Von Recum, A. F.; Grether, M. F.; Coffeen, W. W. Piezoelectric Ceramic Implants: In Vivo Results. *J Biomed Mater Res* **1981**, *15* (1), 103–110.

(28) Jiao, H.; Zhao, K.; Shi, R.; Ma, Y.; Tang, Y.; Bian, T.; Wang, J. An Investigation of the Electrical, Mechanical and Biocompatibility Properties of Barium Titanate/Hydroxyapatite Bulk Ceramics. *Mater Chem Phys* **2020**, *243*, 122613.

(29) Ball, J. P.; Mound, B. A.; Nino, J. C.; Allen, J. B. Biocompatible Evaluation of Barium Titanate Foamed Ceramic Structures for Orthopedic Applications. *J Biomed Mater Res A* **2014**, *102* (7), 2089–2095.

(30) Yaqoob, U.; Uddin, A. S. M. I.; Chung, G.-S. A Novel Tri-Layer Flexible Piezoelectric Nanogenerator Based on Surface-Modified Graphene and PVDF-BaTiO3 Nanocomposites. *Appl Surf Sci* **2017**, *405*, 420–426.

(31) Zhao, Y.; Liao, Q.; Zhang, G.; Zhang, Z.; Liang, Q.; Liao, X.; Zhang, Y. High Output Piezoelectric Nanocomposite Generators Composed of Oriented BaTiO3 NPs at PVDF. *Nano Energy* **2015**, *11*, 719–727. https://doi.org/10.1016/j.nanoen.2014.11.061.

(32) Mohammadpourfazeli, S.; Arash, S.; Ansari, A.; Yang, S.; Mallick, K.; Bagherzadeh, R. Future Prospects and Recent Developments of Polyvinylidene Fluoride (PVDF) Piezoelectric Polymer; Fabrication Methods, Structure, and Electro-Mechanical Properties. *RSC Advances*. Royal Society of Chemistry January 9, 2023, pp 370–387. https://doi.org/10.1039/d2ra06774a.